

**Supporting Information****Pd@MOF-5: Limitations of Gas-Phase Infiltration and Solution Impregnation of [Zn<sub>4</sub>O(bdc)<sub>3</sub>] (MOF-5) with Metal-Organic Palladium Precursors.**

*Daniel Esken,<sup>a</sup> Xiaoning Zhang,<sup>a</sup> Oleg I. Lebedev,<sup>b</sup> Felicitas Schröder,<sup>a</sup> and Roland A. Fischer<sup>a\*</sup>*

<sup>a</sup>Lehrstuhl für Anorganische Chemie II – Organometallics & Materials, Ruhr-Universität Bochum, Universitätsstrasse 150, D-44780, Bochum, Germany.

E-mail: roland.fischer@ruhr-uni-bochum.de;

Fax: (+49) 234 32 14174; Tel: (+49) 234 32 24174.

<sup>b</sup>EMAT, University of Antwerp, Groenenborgerlaan 171, B-2020 Antwerp, Belgium

**Preparation of MOF-5.**

A sample of 3.15 g Zn(NO<sub>3</sub>)<sub>2</sub>·4H<sub>2</sub>O and 0.665 g of terephthalic acid were dissolved into 100 ml diethylformamide (DEF) followed by heating to 105 °C for 24 h. The supernatant was decanted and the deposited cubic crystals were washed three times with fresh DEF (100 mL) and then treated with chloroform (100 mL) for 24 h to exchange the DEF. After decanting the CHCl<sub>3</sub> and washing three times with fresh CHCl<sub>3</sub> (100 mL) the resulting powder was dried at 110 °C in dynamic vacuo (10<sup>-3</sup> mbar) for 12 h. The characterization was done by FT-IR, PXRD, elemental analysis and solid-state NMR spectroscopy. The resulting analytical data and spectra fully agreed with published results. The surface area was determined by N<sub>2</sub> absorption and was calculated with the Langmuir model to 3400 m<sup>2</sup>g<sup>-1</sup>.

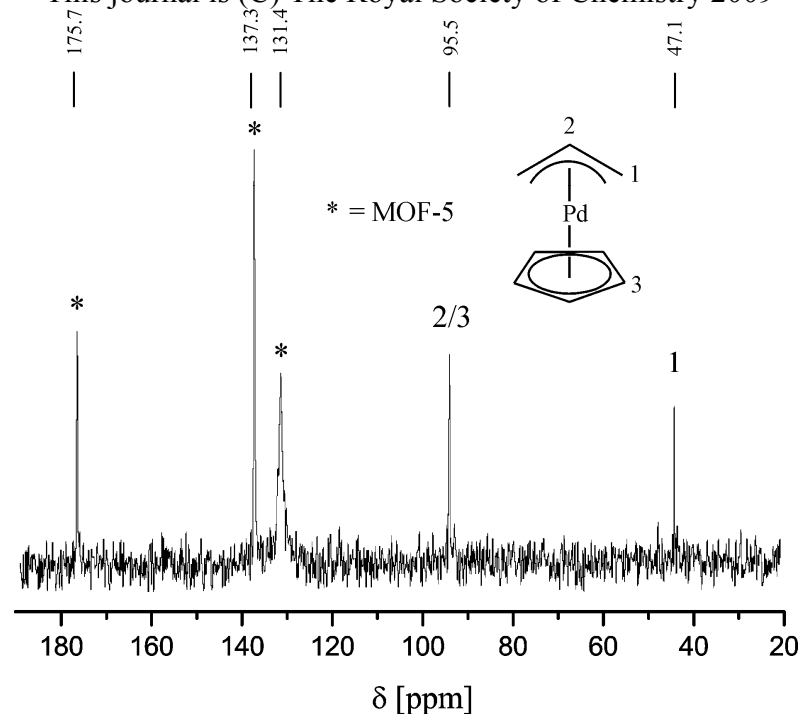


**Figure 1S.**  $^{13}\text{C}$ -CP-MAS NMR spectrum of  $[\text{Pd}(\eta^5\text{-C}_5\text{H}_5)(\eta^3\text{-C}_3\text{H}_5)]_4@\text{MOF-5}$ .

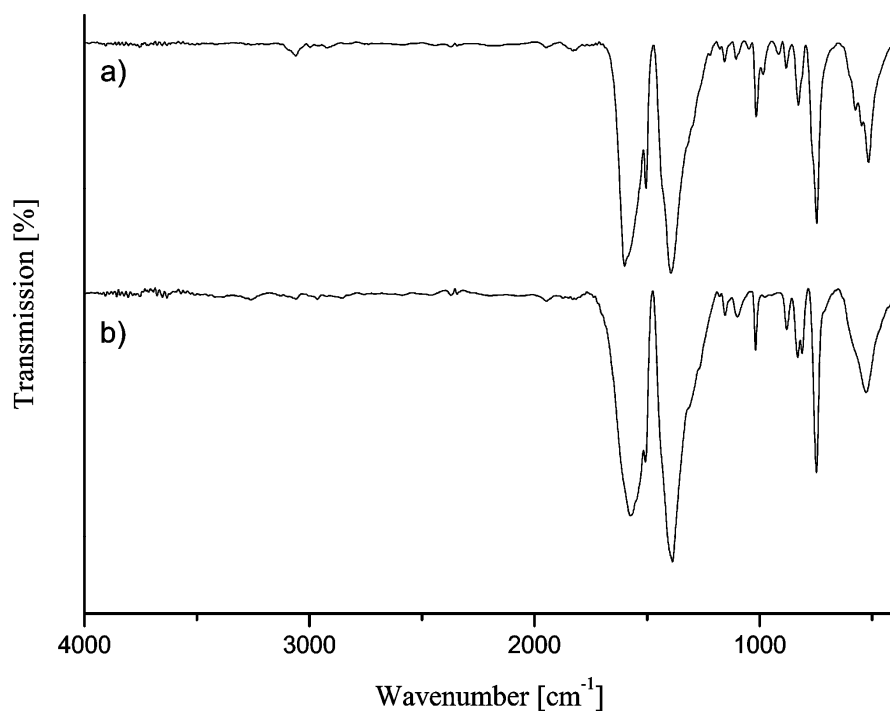


**Figure 2S.** FT-IR spectra of  $[\text{Pd}(\eta^3\text{-C}_3\text{H}_5)(\eta^5\text{-C}_5\text{H}_5)]_4@\text{MOF-5}$  (a) and guest-free MOF-5 (b); additional vibration bands in (a) are derived from precursor inclusion.

**Additional Comment to Figure 1 of the main text.**

The PXRD pattern of the material (Figure 1M, below) shows characteristic reflexes of the host lattice, revealing an intact MOF-5 structure (Figure 1a). In contrast to empty MOF-5 (Figure 1b) some new reflections appear in the diffractogram of the inclusion compound but could not be indexed with respect to a possible adsorbate superstructure of the included molecules similar to  $[\text{Fe}(\eta^5\text{-C}_5\text{H}_5)_2]_7@\text{MOF-5}$ , mentioned above. Note, that the materials  $\text{Pd}_x@\text{MOF-5}$  discussed in our work do not show these few additional peaks in the PXRD pattern. As reported in the related case of  $[\text{Ru}(\text{COD})(\text{COT})]@\text{MOF-5}$  [11], the relative intensities of the first two reflexes of the MOF-5 matrix at low  $2\Theta$  angles of  $6.7^\circ$  and  $9.6^\circ$  are inverted in comparison to the guest-free MOF-5, if the framework is fully loaded with precursor molecules in a very homogenous way. In the present case of  $[\text{Pd}(\eta^5\text{-C}_5\text{H}_5)(\eta^3\text{-C}_3\text{H}_5)]_4@\text{MOF-5}$ , however, a surprisingly small deviation of the initial relative reflex ratio of about 5:1 of MOF-5 is observed in the PXRD experiment (Figure 1). The precursor  $[\text{Pd}(\eta^5\text{-C}_5\text{H}_5)(\eta^3\text{-C}_3\text{H}_5)]$  is not long time stable at room temperature. Some decomposition may have started during the data accumulation and exposure to the X-ray beam, which was indicated by the very dark colour of the sample after the data accumulation.

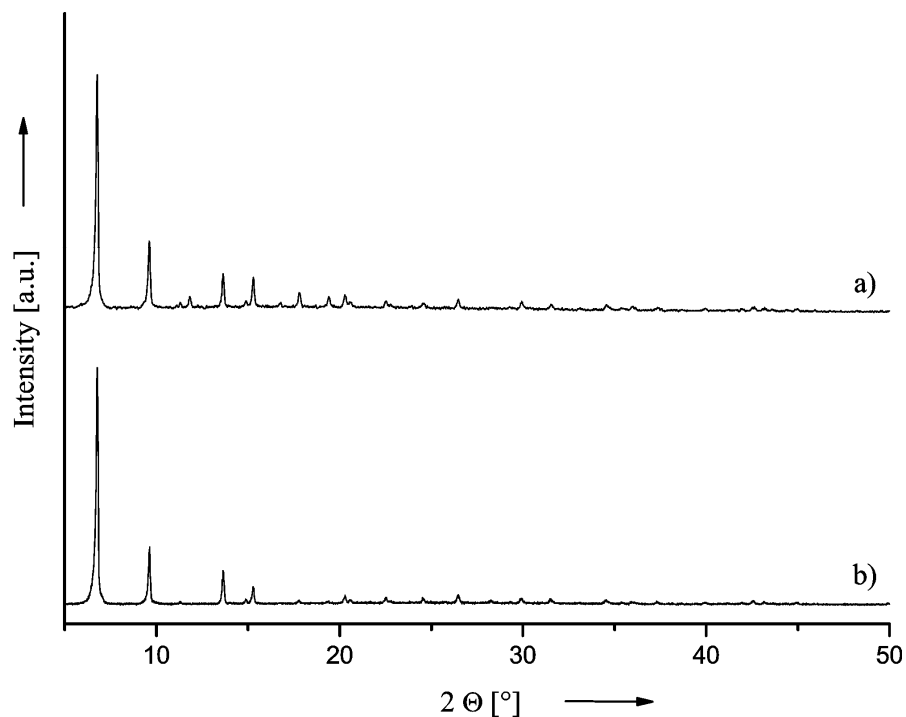


**Figure 1M.** Powder x-ray diffraction pattern of “saturated”  $[\text{Pd}(\eta^5\text{-C}_5\text{H}_5)(\eta^3\text{-C}_3\text{H}_5)]_4@\text{MOF-5}$  (a) and guest-free MOF-5 (b). Note, that a higher loading of  $x > 4$  could in principle be possible, but not at accessible conditions because of the thermal lability of the precursor.

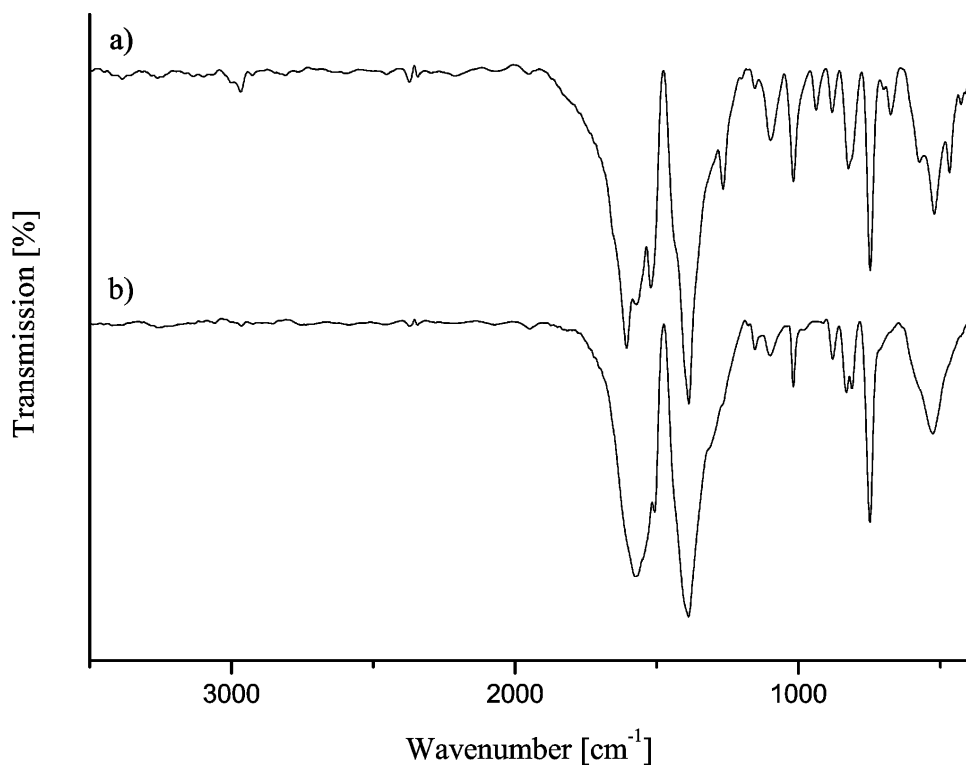


**Figure 3S.** FT-IR spectra of  $[\text{Pd}(\text{acac})_2]_2@\text{MOF-5}$  (a) and guest-free MOF-5 (b); additional vibration bands in (a) are derived from precursor inclusion.

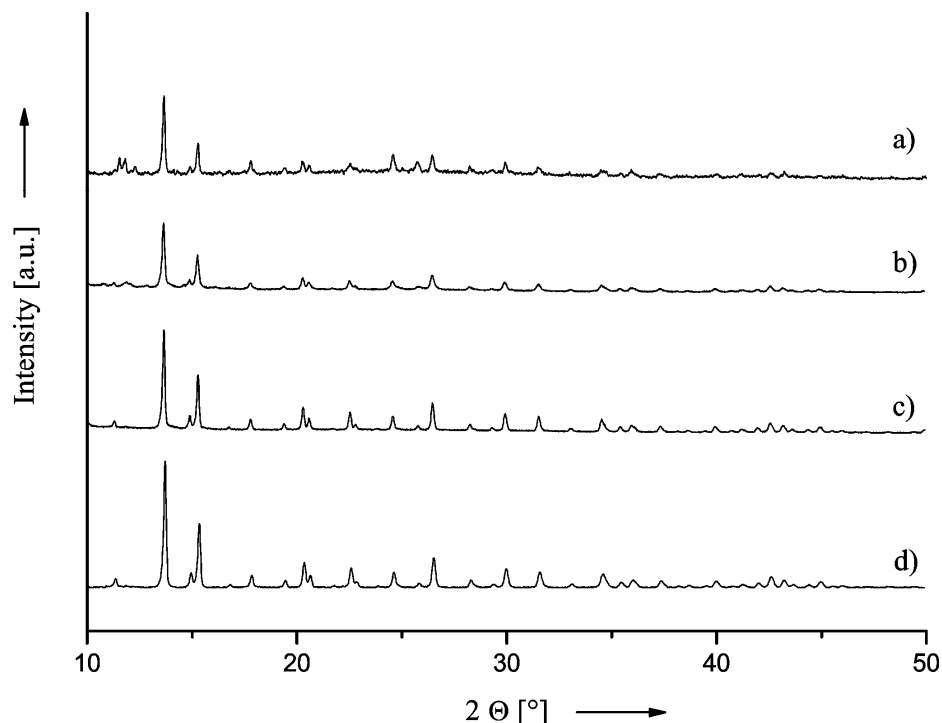


**Figure 4S.** Powder x-ray diffraction pattern of  $[\text{Pd}(\text{acac})_2]_2@\text{MOF-5}$  (a),  $[\text{Pd}(\text{acac})_2]_1@\text{MOF-5}$ ,  $[\text{Pd}(\text{acac})_2]_{0.42}@ \text{MOF-5}$  and guest-free MOF-5 (d)

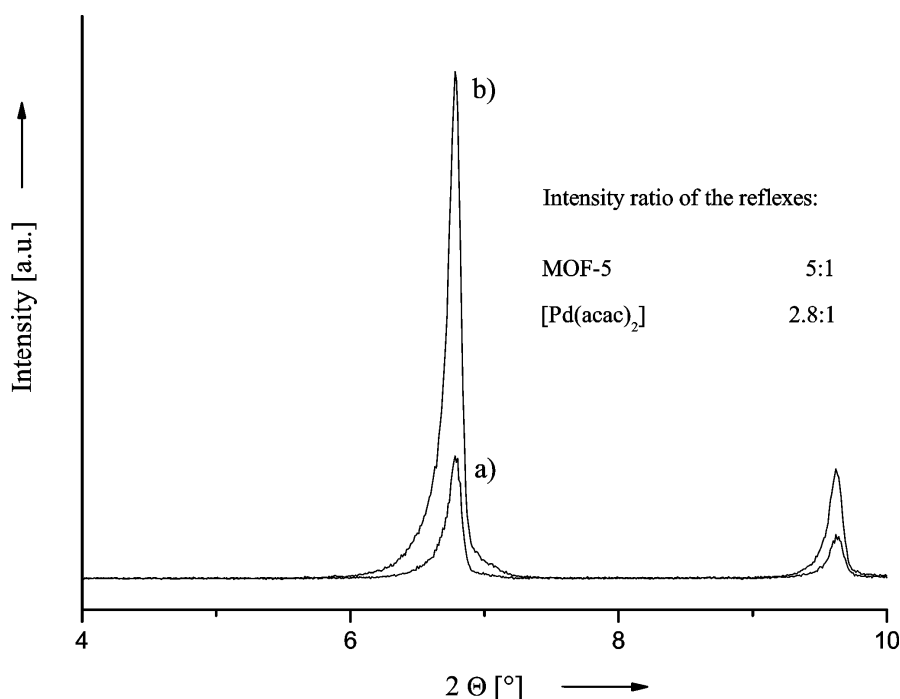


**Figure 5S.** Powder x-ray diffraction pattern of  $[Pd(acac)_2]_2 @ MOF-5$  (a) and guest-free MOF-5 (b); deviation of the relative reflex ratio of the [200] reflex to the [220] reflex gives evidence for pore filling.

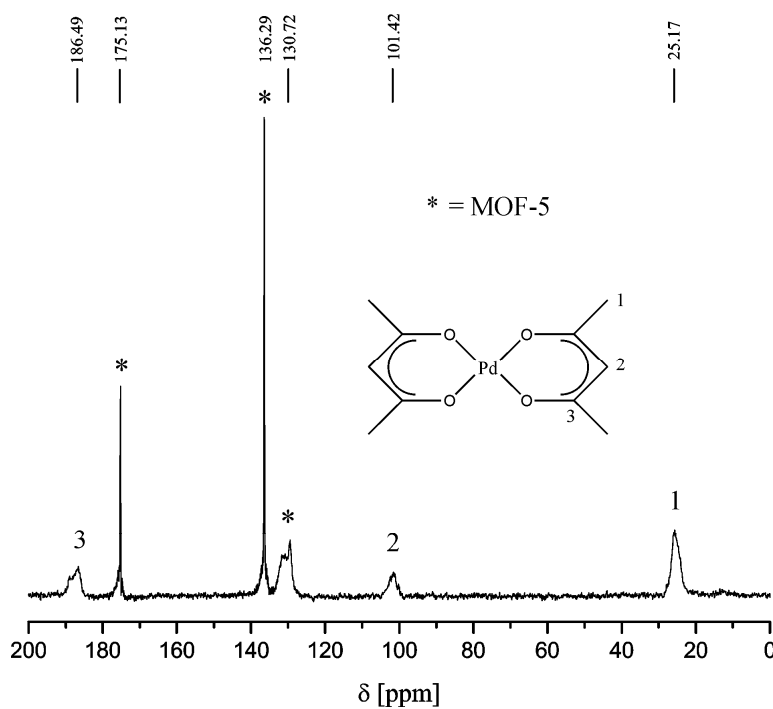


**Figure 6S.**  $^{13}\text{C}$ -CP-MAS NMR spectrum of  $[Pd(acac)_2]_2 @ MOF-5$ .

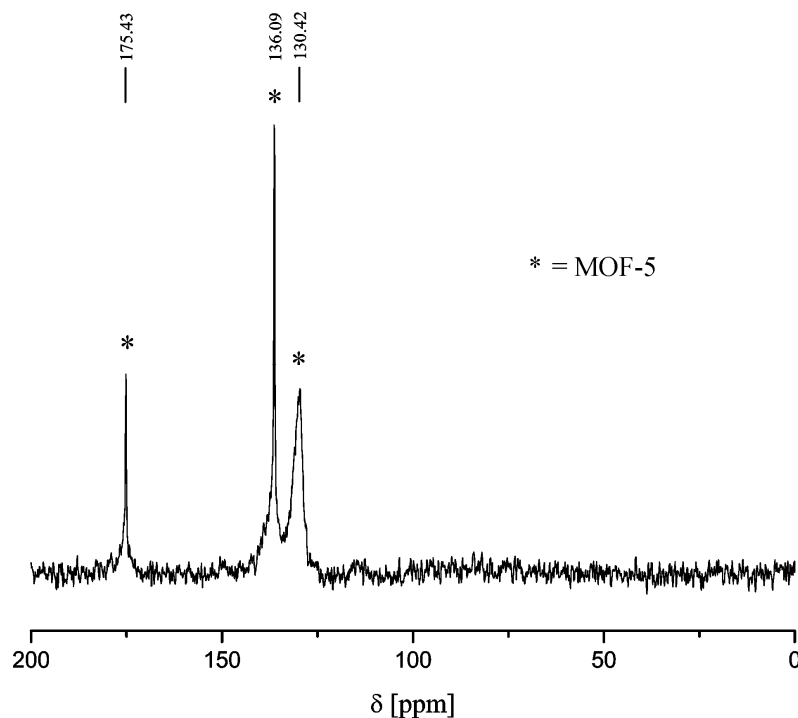


**Figure 7S.** The  $^{13}\text{C}$ -CP-MAS NMR of  $^{\text{h}\nu}\text{Pd}_4@\text{MOF-5}$  after desorption of all volatile ligand fragments shows only characteristic MOF-5 peaks and no signals for  $\text{sp}^3$  carbon atoms.

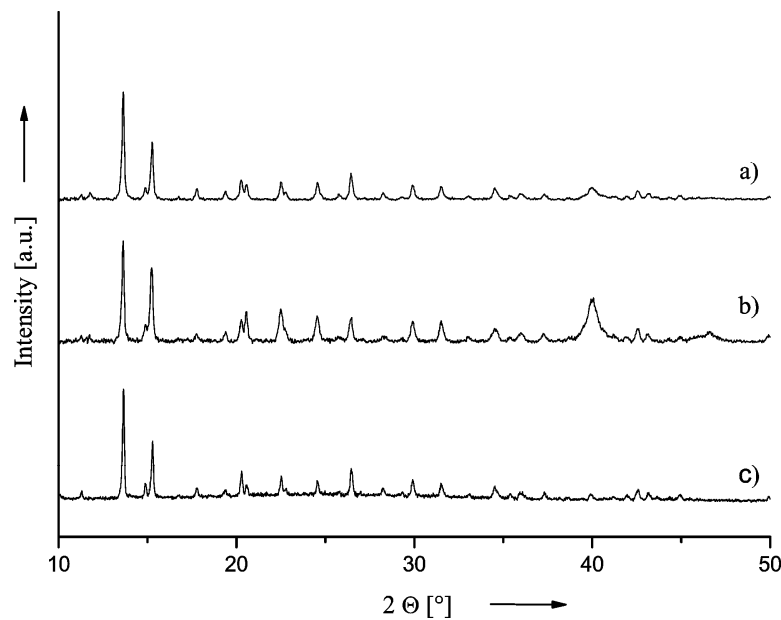


**Figure 8S.** PXRD pattern of hydrogen treated  $\text{Pd}_1@\text{MOF-5}$  (a),  $\text{Pd}_2@\text{MOF-5}$  (b) and guest-free MOF-5 (c); characteristic MOF-5 reflexes confirm the intact network structure. Conditions of hydrogen treatment similar to the samples shown in Figure 7S.

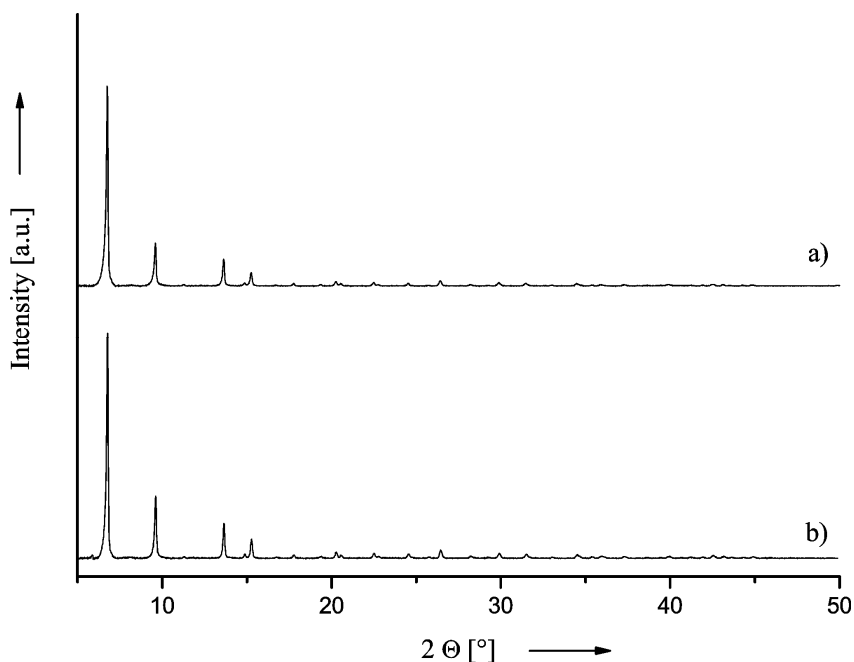


**Figure 9S.** PXRD of  $^{hv}\text{Pd}_4@\text{MOF-5}$ , treated with 2 bar  $\text{H}_2$  at 150 °C for 12 h (a) and freshly prepared  $^{hv}\text{Pd}_4@\text{MOF-5}$  as reference (b).

#### Attempts to further raise the loading of $\text{Pd}_x@\text{MOF-5}$ materials ( $x > 4$ ).

Even in case of high palladium loadings of 35 wt.% ( $x = 4$ ) only a small fraction of the pore volume is loaded with palladium nanoparticles as we have discussed above. An obvious way to further rise the Pd loading, possibly much beyond the reported limiting values of one-step loading procedures, is to repeat the whole loading cycle with a typical pure  $\text{Pd}@\text{MOF-5}$  sample of 20-35 wt.% Pd as the staring material. Surprisingly, we found that the MOF-5 matrix totally collapsed during a second loading cycle irrespectively of the precursor and the method, solvent-free gas-phase or incipient wetness. The PXRD measurements revealed an amorphous material with superimposed palladium peaks (Figure 10S). TEM measurements showed larger particles of  $> 10 \text{ nm}$  (Figure 11S). It is well known from MOCVD, that the growth of Pd thin films from organometallic or metal-organic precursors involves autocatalytic surface processes of palladium nano crystallite growth [29]. We therefore assume a preferred palladium particle growth at the very sites of the particles imbedded in the first loading cycle in competition with independent nucleation and growth at other sites within the MOF-5 matrix. From this observation and considerations we deduce, that a quantitative

loading of *every* cavity of a MOF-5 single crystallite with a *small* Pd nano cluster ( $<< 1.5$  nm) better matching the available space of the cavities will be quite a challenge and will certainly be in severe competition by the preferred rapid growth of Pd particles (Ostwald ripening). The palladium loading of such a hypothetical fully loaded material would range above 90 wt.%. From Pd colloid chemistry it is known, that particle growth can be tuned and even trapped by the choice of suitable surfactants as additives. The additives adsorb at the particle surface typically via -SH, -NH<sub>2</sub>-, -OH or -COOH groups of thiols, amines, alcohols or carboxylic acids [30]. These functional groups however are absent in MOF-5. Consequently, the interaction of the matrix with the Pd nanoparticles is too low to effectively limit the particle growth in a second loading cycle. An obvious way to combine the caging effects of MOF matrices with the surface stabilisation known from surfactants would be the use of suitable functionalized linkers while keeping the MOF structure unchanged. We are currently working in that direction.

29 K. S. Wain, A. Sen and S. H. Kim, *J. Polym. Sci.*, 2005, **43**, 1930.

30 J. Durand, E. Teuma and M. Gómez, *Eur. J. Inorg. Chem.* 2008, **23**, 3577.

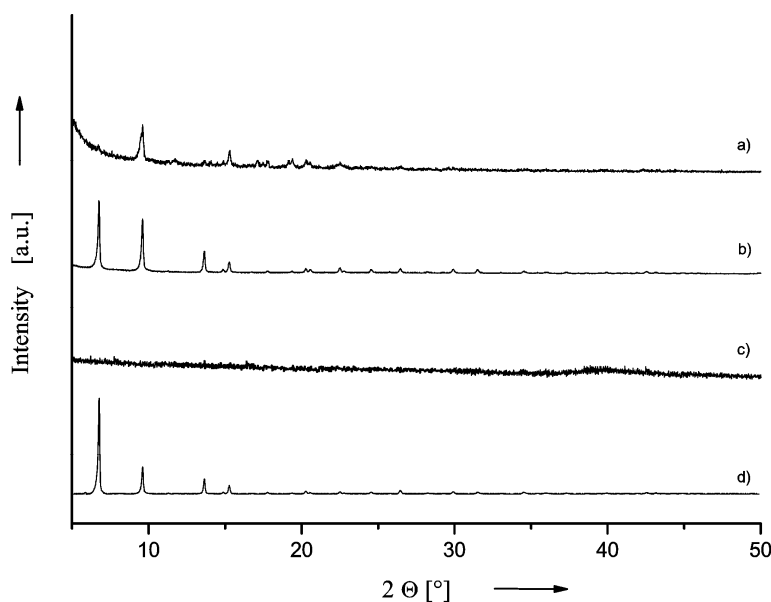


**Figure 10S.** PXRD pattern of <sup>H</sup>Pd<sub>0.07</sub>@MOF-5 (1 wt.% Pd, Table 1 [19]) second loading (a); <sup>H</sup>Pd<sub>0.07</sub>@MOF-5, first loading (b). <sup>hv</sup>Pd<sub>4</sub>@MOF-5, second loading (c) and <sup>hv</sup>Pd<sub>4</sub>@MOF-5, first loading (d).

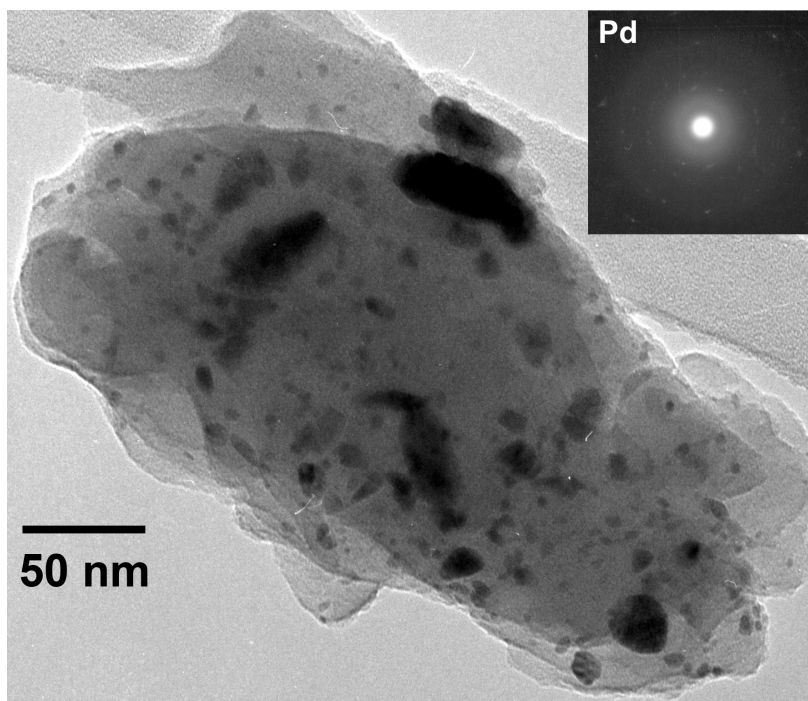


**Figure 11S.** TEM micrograph of a sample  $^H\text{Pd}_{0.07}\text{@MOF-5}$  (Figure 9S b) after a second loading cycle with  $[\text{Pd}(\eta^3\text{-C}_3\text{H}_5)(\eta^5\text{-C}_5\text{H}_5)]$  shows larger particles with a diameter  $> 10 \text{ nm}$ . The SAED pattern confirms the existence of metallic palladium.

#### Hydrogen Stability of as synthesized $^{hv}\text{Pd}_4\text{@MOF-5}$ .

However, when the prolonged hydrogen treatment at  $150^\circ\text{C}$  was done *without* the complete desorption of all the hydrocarbon ligands and species, which are produced by the decomposition of the intercalated palladium precursors during the preparation of the  $\text{Pd}_x\text{@MOF-5}$  materials, the MOF-5 matrix was destroyed. But again, the terephthalic acid linkers were not hydrogenated. Similarly, if  $[\text{Pd}(\eta^5\text{-C}_5\text{H}_5)(\eta^3\text{-C}_3\text{H}_5)]_4\text{@MOF-5}$  is converted into  $^H\text{Pd}_4\text{@MOF-5}$  by thermal hydrogenolysis rather than by photolysis, the MOF-5 matrix will also be significantly damaged [9]. We have no explanation at hand for these facts.